

https://doi.org/10.1070/QEL17606

Effect of transverse displacement of charged particle beams on quantum electrodynamic processes during their collision

M. Filipovic, C. Baumann, A.M. Pukhov, A.S. Samsonov, I.Yu. Kostyukov

Abstract. **Collisions of ultrarelativistic electron beams are considered using full-scale 3D particle-in-cell simulation. In this process, the particles can be affected by the superintense fields of the counterpropagating beam, and the interaction can pass to the regime of nonperturbative quantum electrodynamics. In this experimentally unexplored regime, the emission of photons and the production of electron–positron pairs are extremely probable processes. It is shown that due to the transverse displacement of the beams and an increase in the number of particles located in the region of the field maximum, it is possible to increase the yield of both photons and electron–positron pairs.**

Keywords: *collider, ultrarelativistic case, photon emission, pair production, particle-in-cell simulation.*

In connection with the rapid development of technologies for constructing high-power lasers, in the foreseeable future, it is expected to achieve laser radiation intensities exceeding 10^{22} W cm^{-2} [1–5], which will allow the laser radiation–matter interaction to be experimentally studied at very high energies. One of the directions of the research is the investigation of quantum electrodynamic (QED) effects in a strong field. QED processes can be classified by the quantum parameter $\chi = \sqrt{-(F_{\mu\nu}p^{(\nu)})^2}/(m_e c E_{cr})$ [6], where E_{cr} is the critical field of vacuum breakdown [7], or the Schwinger limit; $F_{\mu\nu}$ is the electromagnetic field tensor; m_e is the rest mass of an electron; c is the speed of light in vacuum; and $p^{(\nu)}$ is the four-dimensional momentum. The parameter χ allows quantifying the effect of QED processes on the interaction of radiation with matter, the most important of which are the emission of hard photons due to nonlinear Compton scattering and the generation of electron–positron pairs due to the Breit–Wheeler multiphoton process [6, 8]. When the parameter χ reaches a value of the order of unity, the probabilities of these processes become significant.

M. Filipovic, C. Baumann Institut für Theoretische Physik I, Heinrich-Heine-Universität Düsseldorf, 40225 Düsseldorf, Germany;
A.M. Pukhov Institut für Theoretische Physik I, Heinrich-Heine-Universität Düsseldorf, 40225 Düsseldorf, Germany; Lobachevsky State University of Nizhny Novgorod, prosp. Gagarina 23, 603950 Nizhny Novgorod, Russia;
A.S. Samsonov, I.Yu. Kostyukov Lobachevsky State University of Nizhny Novgorod, prosp. Gagarina 23, 603950 Nizhny Novgorod, Russia; Institute of Applied Physics, Russian Academy of Sciences, ul. Ulyanova 46, 603950 Nizhny Novgorod, Russia;
e-mail: asams@ipfran.ru

Received 8 July 2021
Kvantovaya Elektronika **51** (9) 807–811 (2021)
Translated by V.L. Derbov

The regime at $\chi < 1$ was implemented in the E-144 experiment at the SLAC facility [9], and it is expected that the regime at $\chi \approx 1$ will be realised in the E-320 experiment at the SLAC facility [10] and in the LUXE experiment at the DESY facility [11]. No less important is the study of the so-called 'supercritical regime' corresponding to the limit $\chi \gg 1$ [12]. The theory predicts that if the parameter χ becomes large enough to satisfy the condition $\alpha\chi^{2/3} \geqslant 1$, where α is the fine structure constant, then the mentioned QED processes are so significant that the QED theory turns out to be nonperturbative [13]. Not only this regime has not been studied experimentally, but there is also no reliable QED theory, since in this regime the expansion parameter in the QED perturbation theory ceases to be small. Nevertheless, possible schemes for implementing this regime in an experiment have already been proposed [14–17] and some preliminary analytical studies have been performed [18–22].

One of the biggest problems to be solved in order to achieve a fully nonperturbative QED regime is minimising the energy losses of particles before they enter the strong field region, in which the condition $\alpha\chi^{2/3} \geqslant 1$ is satisfied. Simple estimates show that schemes based on collisions of a laser pulse with an electron beam are not viable, since even for the parameters of laser radiation that are expected to be obtained at facilities with a peak power of 10 PW, electron bunches with a Lorentz factor of $\gamma \approx 10^7$ are required. An alternative configuration using a 100 GeV-class electron collider is more promising [23]. In this paper, we propose a development of this scheme of an electron–electron collider. In particular, the collision of electron beams displaced with respect to each other in the transverse direction is considered to ensure a higher yield of secondary particles as a result of QED processes. In addition, the energy losses with an increase in the length of electron bunches are discussed, and the yield of secondary particles is compared with the previous analytical estimates [24, 25].

To study the collision of beams, we performed a numerical simulation by the particle-in-cell (PIC) method using the virtual laser plasma laboratory (VLPL) code [26] in three-dimensional geometry. The simulation domain was $20\sigma_0$, $30\sigma_0$, and $30\sigma_0$ along the x, y, and z axes, respectively, where $\sigma_0 = 10$ nm is the characteristic spatial size used for normalisation in each simulation. The grid steps were $0.025\sigma_0$, $0.1\sigma_0$, and $0.1\sigma_0$ along the same axes. The time step was equal to the step value in the direction of the x axis, which was dictated by the choice of the rhombi-in-plane (RIP) pattern [27] for the numerical solution of Maxwell's equations. The diameter and length of the beams were 10 nm (unless indicated otherwise), the peak current was $I_{max} = 1.7$MA, the Lorentz factor of the particles was $\gamma = 2.5 \times 10^5$, and a Gaussian ellipsoid was used

as the density profile. For all the calculations performed, the transverse boundary conditions were periodic, and the longitudinal ones were absorbing. QED processes in this code are simulated using the Monte Carlo method [28, 29]. In the calculations performed, two QED processes were taken into account – the nonlinear Compton scattering and the Breit–Wheeler process. In this paper, two possible configurations are considered. In the first configuration, hereinafter called 'undisplaced', the transverse positions of the centres of the two electron beams coincide. The second configuration, called 'displaced', is schematically shown in Fig. 1. In this case, one of the two electron beams is displaced relative to the other in the direction of the y axis by a distance d_0. This distance is chosen such that the density maximum of one electron beam passes through the electric field maximum of the counterpropagating beam. The expression for the electric field strength can be found from the Gauss theorem:

$$\boldsymbol{E} = -\frac{4\pi\sigma_r^2 n_0 e}{r}\exp\left[-\frac{(x-vt)^2}{2\sigma_x^2}\right] \times\left[1-\exp\left(-\frac{r^2}{2\sigma_r^2}\right)\right]\boldsymbol{e}_r, \quad (1)$$

where σ_r is the root-mean-square beam radius; σ_x is the root-mean-square length of the beam (note that below the results of modelling with different beam lengths σ_x will be presented); $v \approx c$ is the speed of the beam particles; and n_0 is the maximum concentration of beam particles [30]. For the above simulation parameters, the maximum electric field $E_{\max} = 13.8(2\pi m_e c^2) \times (e\sigma_0)^{-1}$ is achieved at $r_{\max} \approx 1.59\sigma_r$. Thus, the optimal shift for the displaced configuration is $d_0 = r_{\max} \approx 15.9$ nm.

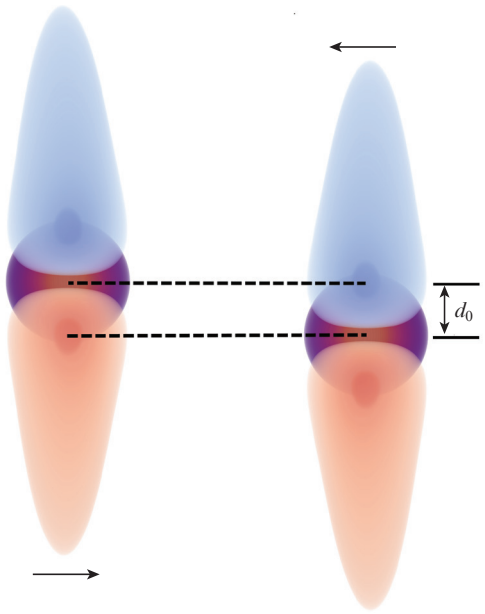

Figure 1. (Colour online) Modified collision configuration of electron bunches: the electron density (purple and yellow) at the beginning of the simulation, the y-component of the electric field (red-blue colour scheme).

First of all, we found that, in the simulation, the interaction actually occurs in a nonperturbative QED regime, realised under the condition $\alpha\chi^{2/3} \geqslant 1$, or $\chi \geqslant 1600$. Figure 2 shows the maximum values of the parameter χ in the yz plane at complete overlap of both bunches. Large χ values are observed in a ring around the bunch propagation axis for an undisplaced configuration (Fig. 2a) and in two rings for a displaced configuration (Figs 2b, 2c). The reason for this distribution of the parameter χ is related to its dependence on the strength of the electric field, which has axial symmetry and possesses a maximum at some distance from the centre of the beam [see Eqn (1)]. The maximum value of χ is 1695 in both configurations, which confirms the implementation of a completely nonperturbative QED regime. An estimate shows that in an undisplaced configuration, about 34% of the beam electrons reach this regime. This value is in agreement with the estimate obtained by Yakimenko et al. [23]. For comparison, the fraction of electrons reaching the supercritical regime in the displaced configuration is about 33%. Despite this, in the displaced configuration, the yield of both photons and electron–positron pairs is higher (see below). This spatial distribution of the parameter χ directly affects the QED processes. In particular, Fig. 3 shows the energy density distributions of the emitted photons in both configurations. Since the probability of photon emission is related to the value of the parameter χ, in the undisplaced configuration the emitted photons are located symmetrically around the beam propagation axis and are almost absent in a small channel along the x axis. In the displaced configuration, the photons are located near the axes of propagation of both beams because the centres of the beams lie in the region of the maximum electric field. Before further analysis of the simulation results, we present the estimates of the secondary particle yield obtained in [24]. It shows that the ratio of the total number of photons to the initial number of electrons in the bunch can be expressed in terms of the average value of the parameter χ, which is analytically calculated for the Gaussian distribution of the beam concentration as follows:

$$\chi^{\text{av}} = \Upsilon \approx \frac{5}{12}\frac{N_{e0}\alpha\gamma\lambda_C^2}{\sigma_r\sigma_x}, \quad (2)$$

where N_{e0} is the initial number of electrons in the bunch, and λ_C is the reduced Compton wavelength. With the chosen interaction parameters and a bunch charge of 0.14 nC, the parameter Υ is equal to 990. The average value χ^{av} of the parameter χ, calculated from the results of numerical simulation, was ~790 in the undisplaced configuration and ~787 in the displaced configuration at the moment of the complete overlapping of the beams. Since the parameter χ^{av} is determined by the field of each beam, its values are close in both configurations. In the limit $\Upsilon \gg 1$, the ratio of the number of photons to the initial number of electrons in the bunch can be estimated as

$$\frac{N_\gamma}{N_{e0}} \approx 2.57\left(\frac{\sigma_x}{\gamma\lambda_C}\alpha\Upsilon^{2/3}\right). \quad (3)$$

Substitution of the value of the parameter χ^{av} into this formula gives the ratio $N_\gamma/N_{e0} \approx 0.193$, which is in good agreement with the simulation results, according to which this ratio is ~0.203 for the undisplaced configuration and ~0.210 for the displaced one. It is also possible to estimate the energy

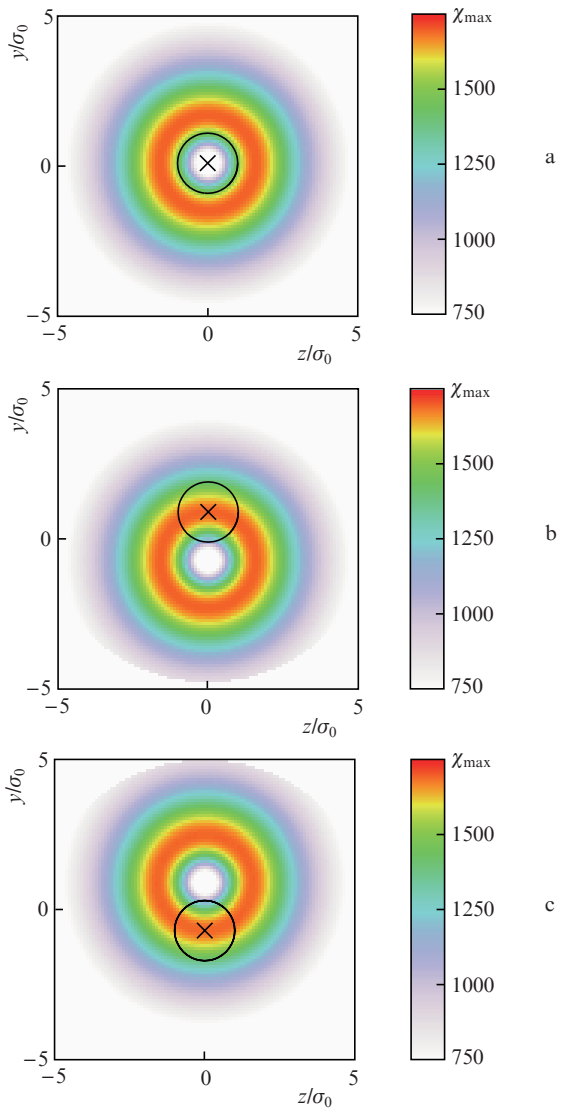

Figure 2. (Colour online) Maximum values of the parameter χ in the simulation domain with complete overlap of bunches in the yz plane for (a) an undisplaced configuration, as well as for the electron beam moving (b) to the right and (c) to the left in a displaced configuration. The crosses show the position of the beam centre, and the black circle with radius σ_r is the size of the beam.

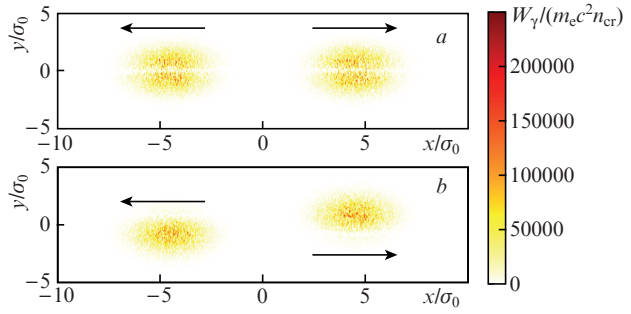

Figure 3. (Colour online) Energy density of emitted photons in the xy plane after collision of electron bunches in (a) undisplaced and (b) displaced configurations. Arrows indicate the direction of propagation of photon bunches; W_γ is the photon energy density in the simulation cell, n_{cr} is the critical density calculated for a frequency corresponding to a wavelength of 1 nm.

losses ε_e, which are directly related to the emission of photons by electrons [24]:

$$\frac{\Delta\varepsilon_e}{\varepsilon_e} \approx -0.689\left(\frac{\sigma_x}{\gamma\lambda_C}\alpha\Upsilon^{2/3}\right). \tag{4}$$

According to this estimate, the energy loss is $\Delta\varepsilon_e/\varepsilon_e \approx 5.18\%$ for the parameters used in the numerical simulation. This estimate also agrees well with the results of numerical simulations, in which $\Delta\varepsilon_e/\varepsilon_e \approx 5.01\%$ in the undisplaced configuration and $\sim 5.14\%$ in the displaced configuration.

Similar estimates can be made for another QED process under consideration, namely, the production of electron–positron pairs from photons emitted by electrons. In Ref. [25], the ratio of the number of produced electron–positron pairs to the initial number of electrons in the bunch was estimated as

$$\frac{N_{pairs}}{N_{e0}} \approx \frac{10.4\sqrt{3}}{25\pi}\left(\frac{\sigma_x}{\gamma\lambda_C}\alpha\Upsilon^{2/3}\right)^2 \ln\Upsilon \tag{5}$$

for $\Upsilon \gg 1$. For the simulation parameters, this estimate gives the ratio $N_{pairs}/N_{e0} \approx 0.0089$, which is in good agreement with the results of numerical simulations, according to which $N_{pairs}/N_{e0} \approx 0.0084$ in the undisplaced configuration and ~ 0.0087 in the displaced one.

We also studied the effect of the beam length on the applicability of analytical estimates. To this end, a series of numerical simulations was carried out for the beam length varying with a step of 10 nm. In this case, the maximum concentration of electrons and bunch size σ_r were the same as in the simulation described above. Figure 4a shows the ratios of the number of photons to the initial number of electrons in the bunch, obtained as a result of numerical simulation and using analytical estimate (3) under the assumption that $\chi^{av} = \Upsilon$. It can be seen that in both configurations the photon yield increases with increasing beam length, and hence the bunch interaction time. The energy losses and the yield of electron–positron pairs shown in Figs 4b and 4c, respectively, reflect the same regularity. The simulation results show that the simultaneous displacement of the beam centres and increase in their length generally increase the yield of secondary particles. Thus, in the displaced configuration for beams with a length of 10 nm, the photon yield increases by $\sim 3.3\%$, and the yield of electron–positron pairs by $\sim 4.4\%$ compared to the undisplaced configuration, while for beams with a length of 50 nm, the increase is $\sim 5.4\%$ for photons and $\sim 4.9\%$ for pairs. It should be noted that the simulation results and analytical estimates are in good agreement for short bunches, but slightly differ for longer bunches. It can be seen from Fig. 4 that, although analytical estimates still give the correct order of magnitude for beams with a length greater than 30 nm, the predicted functional dependence is somewhat different from that observed in the simulation. This is partly explained by the fact that with increasing beam lengths the transverse dynamics of particles becomes important.

The average values of the transverse momentum of the initial electrons after a complete crossing of the beams are presented in Table 1, from which follows the direct dependence of this quantity on the beam length. With an increase in the transverse momentum of the beam particles, the change in the charge distribution in the beam becomes more significant, which, in turn, leads to a change in the distribution of the electromagnetic field. This causes the discrepancy between

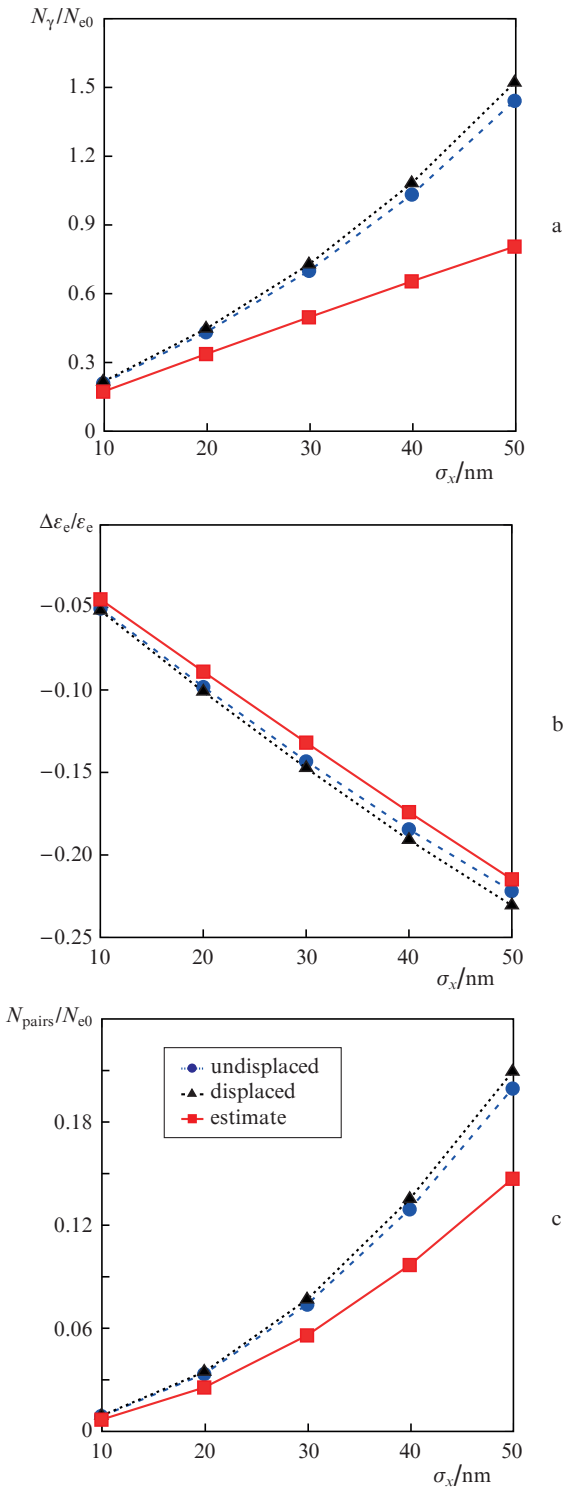

Figure 4. (Colour online) Ratio of the number of emitted photons to the initial number of electrons (a), the energy losses by electrons (b), and the ratio of the number of electron–positron pairs to the initial number of electrons (c) as functions of the beam length. The red curves are based on estimates (3)–(5) and the value of χ^{av} calculated from the simulation results.

the analytical estimates, which were obtained under the assumption that the field distribution remains unchanged, with the results of modelling the collision of extended beams. An influence of transverse particle dynamics on collisions of beams is studied in detail in Ref. [31].

Table 1. The average value of the transverse momentum $p_\perp^{av}$ of the initial electrons after a complete overlap of the beams in different configurations for different beam lengths (p_0 is the initial momentum).

Beam length σ_x/nm	$1000\, p_\perp^{av}/p_0$	
	undisplaced configuration	displaced configuration
10	0.69	0.72
20	1.36	1.39
30	1.97	2.02
40	2.51	2.59
50	2.97	3.10

In addition, we observed the effect of the displacement of the beams on the energy of secondary particles. Figure 5 shows the energy spectrum of positrons in both configurations for bunches with a length of σ_x = 50 nm. One can see that the displaced configuration contains a greater number of low-energy positrons than the undisplaced one.

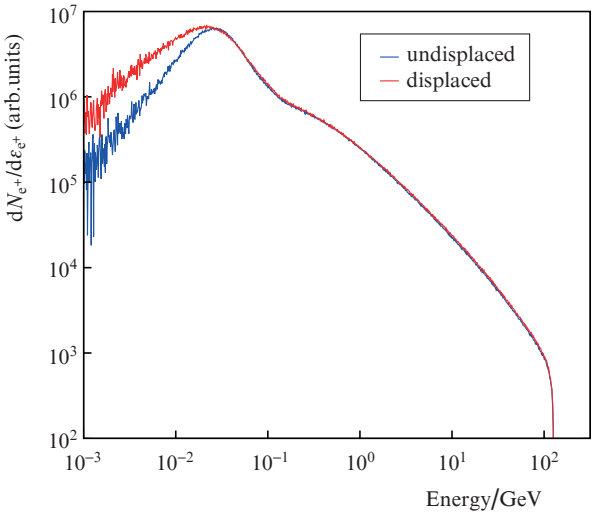

Figure 5. (Colour online) Double logarithmic spectrum of positrons after complete interaction of 50 nm bunches in both configurations.

Thus, in this work, we propose an improvement to the configuration described in [23] aimed at increasing the particle yield while maintaining the nonperturbative QED regime. We considered a collision of electron bunches displaced across their axes so that the maximum density of one bunch passes through the maximum of the field of the counterpropagating bunch. It was found that in this configuration, a higher yield of both photons and electron–positron pairs is observed than in the collision of undisplaced beams. The study was carried out using 3D particle-in-cell simmulation. Comparison of the results obtained with the results of previous works, in which analytical estimates of the particle number yield were obtained, shows that these estimates are in good agreement with the results of numerical simulation in the case of short beams, but somewhat differ in the case of long beams, when the transverse dynamics of particles becomes essential.

Acknowledgements. This work was supported by Deutsche Forschungsgemeinschaft (DFG) (Project 430078384) and the Russian Science Foundation (Grant No. 18-11-00210; analy-

sis of simulation results and comparison with analytical estimates). The authors gratefully acknowledge the Gauss Centre for Supercomputing e.V. (www.gauss-centre.eu) for funding this project (qed20) by providing computing time on the GCS Supercomputer JUWELS at Jülich Supercomputing Centre (JSC).

References

1. Yoon J.W., Kim Y.G., Choi I.W., Sung J.H., Lee H.W., Lee S.K., Nam C.H. *Optica*, **8**, 630 (2021).
2. The ELI Project; http://www.eli-laser.eu.
3. Exawatt Center for Extreme Light Studies (XCELS); https://xcels.ipfran.ru.
4. Zou J.P., Le Blanc C., Papadopoulos D., Chériaux G., Georges P., Mennerat G., Druon F., Lecherbourg L., Pellegrina A., Ramirez P. *High Power Laser Sci. Eng*., **3**, e2 (2015).
5. Hernandez-Gomez C., Blake S.P., Chekhlov O., Clarke R.J., Dunne A.M., Galimberti M., Hancock S., Heathcote R., Holligan P., Lyachev A., Matousek P., Musgrave I.O., Neely D., Norreys P.A., Ross I., Tang Y., Winstone T.B., Wyborn B.E., Collier J. *J. Phys. Conf. Ser*., **244**, 032006 (2010).
6. Di Piazza A., Müller C., Hatsagortsyan K.Z., Keitel C.H. *Rev. Mod. Phys*., **84**, 1177 (2012).
7. Schwinger J. *Phys. Rev*., **82**, 664 (1951).
8. Narozhny N.B., Fedotov A.M. *Contemp. Phys*., **56**, 249 (2015).
9. Bula C., McDonald K.T., Prebys E.J., Bamber C., Boege S., Kotseroglou T., Melissinos A.C., Meyerhofer D.D., Ragg W., Burke D.L., Field R.C., Horton-Smith G., Odian A.C., Spencer J.E., Walz D., Berridge S.C., Bugg W.M., Shmakov K., Weidemann A.W. *Phys. Rev. Lett*., **76**, 3116 (1996).
10. Meuren S., Bucksbaum P.H., Fisch N.J., Fiúza F., Glenzer S., Hogan M.J., Qu K., Reis D.A., White G., Yakimenko V. ArXiv Preprint. ArXiv2002.10051 (2020).
11. Abramowicz H., Acosta U.H., Altarelli M., et al. ArXiv Preprint. ArXiv1912.07508 (2019).
12. Tamburini M., Meuren S. ArXiv Preprint. ArXiv1912.07508 (2019).
13. Narozhny N.B. *Phys. Rev. D*, **21**, 1176 (1980).
14. Blackburn T.G., Ilderton A., Marklund M., Ridgers C.P. *New J. Phys*., **21**, 053040 (2019).
15. Baumann C., Nerush E.N., Pukhov A., Kostyukov I.Y. *Sci. Rep*., **9**, 9407 (2019).
16. Baumann C., Pukhov A. *Plasma Phys. Controlled Fusion*, **61**, 074010 (2019).
17. Di Piazza A., Wistisen T.N., Tamburini M., Uggerhøj U.I. *Phys. Rev. Lett*., **124**, 044801 (2020).
18. Podszus T., Di Piazza A. *Phys. Rev. D*, **99**, 076004 (2019).
19. Fedotov A. *J. Phys. Conf. Ser*., **826**, 012027 (2017).
20. Ilderton A. *Phys. Rev. D*, **99**, 085002 (2019).
21. Mironov A.A., Meuren S., Fedotov A.M. *Phys. Rev. D*, **102**, 053005 (2020).
22. Ekman R., Heinzl T., Ilderton A. *Phys. Rev. D*, **102**, 116005 (2020).
23. Yakimenko V., Meuren S., Del Gaudio F., Baumann C., Fedotov A., Fiuza F., Grismayer T., Hogan M.J., Pukhov A., Silva L.O., White G. *Phys. Rev. Lett*., **122**, 190404 (2019).
24. Yokoya K., Chen P. *Beam-Beam Phenomena in Linear Colliders* (Springer, 1992).
25. Chen P., Telnov V.I. *Phys. Rev. Lett*., **63**, 1796 (1989).
26. Pukhov A. *J. Plasma Phys*., **61**, 425 (1998).
27. Pukhov A. *J. Comput. Phys.*, **418**, 109622 (2020).
28. Elkina N.V., Fedotov A.M., Kostyukov I.Y., Legkov M.V., Narozhny N.B., Nerush E.N., Ruhl H. *Phys. Rev. Spec. Top. Accel. Beams*, **14**, 054401 (2011).
29. Baumann C., Pukhov A. *Phys. Rev. E*, **94**, 063204 (2016).
30. Del Gaudio F., Grismayer T., Fonseca R.A., Mori W.B., Silva L.O. *Phys. Rev. Accel. Beams*, **22**, 023402 (2019).
31. Samsonov A.S., Nerush E.N., Kostyukov I.Yu., Filipovic M., Baumann C., Pukhov A. ArXiv Preprint. ArXiv:2107.04787 (2021)